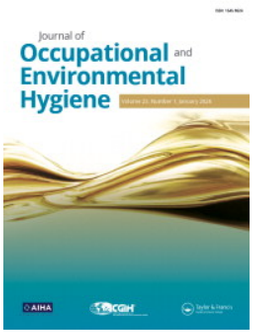

Taylor & Francis
Taylor & Francis Group

Journal of Occupational and Environmental Hygiene

ISSN: 1545-9624 (Print) 1545-9632 (Online) Journal homepage: www.tandfonline.com/journals/uoeh20

Activated carbon fiber (ACF) as a dual respirator media for particulate matter (PM) filtration and volatile organic compound (VOC) adsorption

Brie M. McMahan, Jonghwa Oh, Renjith Pillai, Vinoy Thomas, Mary Appah & Claudiu T. Lungu

To cite this article: Brie M. McMahan, Jonghwa Oh, Renjith Pillai, Vinoy Thomas, Mary Appah & Claudiu T. Lungu (21 Jan 2026): Activated carbon fiber (ACF) as a dual respirator media for particulate matter (PM) filtration and volatile organic compound (VOC) adsorption, Journal of Occupational and Environmental Hygiene, DOI: 10.1080/15459624.2025.2602760

To link to this article: https://doi.org/10.1080/15459624.2025.2602760

Published online: 21 Jan 2026.

JOURNAL OF OCCUPATIONAL AND ENVIRONMENTAL HYGIENE
https://doi.org/10.1080/15459624.2025.2602760

Taylor & Francis
Taylor & Francis Group

Activated carbon fiber (ACF) as a dual respirator media for particulate matter (PM) filtration and volatile organic compound (VOC) adsorption

Brie M. McMahan[a], Jonghwa Oh[a], Renjith Pillai[b], Vinoy Thomas[c], Mary Appah[d], and Claudiu T. Lungu[a]

[a]Department of Environmental Health Sciences, School of Public Health, University of Alabama at Birmingham, Birmingham, Alabama; [b]Research and Development, Creative Polymer Solutions, Birmingham, Alabama; [c]Department of Mechanical and Materials Engineering, School of Engineering, University of Alabama at Birmingham, Birmingham, Alabama; [d]Department of Biostatistics, School of Public Health, University of Alabama at Birmingham, Birmingham, Alabama

ABSTRACT

Exposure to volatile organic compounds (VOCs) and particulate matter (PM) can cause adverse health effects such as pneumoconiosis-like symptoms, acute toxicity, and carcinogenesis. The present work aimed to test activated carbon fiber (ACF) as air-purifying media capable of dual-protection from both PM and VOC and evaluated the interaction between filtration efficiency (FE) and VOC retention by using breakthrough times. The first set of experiments exposed ACF 1200 (1,200 m^2/g nominal surface area) to the VOC toluene at the permissible exposure limit (200 ppm) prior to introducing PM (NaCl, 200 mg/m^3) into the airstream, and the second set of experiments introduced VOC into the airstream after PM exposure. Study findings suggest that ACF 1200 demonstrated a somewhat greater adsorption capacity (g/g) for toluene when PM was present, recording a value of 0.319 g/g, compared to 0.213 g/g in its absence. A slight decline in FE was observed in 1, and 4-layer combinations following initial exposure to VOCs. These findings suggest that the presence of PM may enhance ACFs' adsorption of VOCs; however, the presence of toluene seemed to affect ACF filtration performance to a lesser degree. Understanding these interactions is necessary for the ongoing development of ACF as dual respirator media for both PM and VOCs.

KEYWORDS

Adsorption; aerosols; filtration; occupational hygiene; respiratory protection

Introduction

Millions of workers in the United States rely on respiratory protection for their safety to perform various duties. The use of respiratory protection devices (RPDs) is crucial in the industrial, healthcare, and first responder/emergency management sectors (National Academies of Sciences, Engineering, and Medicine 2022). Inhalation of particulate matter (PM) and/or volatile organic compounds (VOCs) can lead to short- and long-term health effects including acute toxicity, carcinogenesis, chronic bronchitis, obliterative bronchiolitis (OB), chronic obstructive pulmonary disease (COPD), emphysema, and an increased risk of cardiovascular diseases such as heart attacks (Kogevinas et al. 2007; Bernstein and Suojalehto 2011). A global study on occupational respiratory diseases estimated that in 2016, there were approximately 519,000 deaths related to occupational exposures to PM, vapors, and fumes. North America alone contributed to about 20% of these occupational respiratory disease deaths worldwide, with an estimated 104,695 deaths (Kogevinas et al. 2007; Hamanaka and Mutlu 2018; Collaborators GOCRRF 2020; Bernstein and Suojalehto 2011).

Many workers in industrial settings come into contact with aerosols and solvent vapors, especially during cleaning, application of spray coatings (Jayjock and Levin 1984; Gutierrez et al. 2014; Pongboonkhumlarp and Jinsart 2022), or while working near the steel curing processes in a foundry (Chen et al. 2011). Aerosols produced during the curing of steel and spray painting in the automotive industry are a blend of solvents and PM that may cause inflammatory responses in the respiratory system. Studies have indicated that workplaces where individuals are exposed to solvent vapors emitted from paints and adhesives have a strong correlation with the development of COPD (Tagiyeva et al. 2017). The circumstances become increasingly concerning in working environments where workers encounter both aerosol (Chinn M et al. 2002; Chinn MHC and

CONTACT Claudiu T. Lungu clungu@uab.edu Department of Environmental Health Sciences, School of Public Health, University of Alabama at Birmingham, Birmingham, AL.

Pears, L. 2002; Lorimier et al. 2008) particles and solvent vapors at the same time, as the interaction of these exposures could exacerbate respiratory health problems (Shiraiwa et al. 2017). Current practices predominantly feature respirators specifically tailored for PM or organic vapors (OV).

There is a limited selection of respirators that offer dual protection against both types of hazards. Among the different types of respiratory protection, non-powered air purifying respirators (APRs), powered air-purifying respirators (PAPR), and pancake style respirators (typically used with reusable elastomeric respirators) have all been recognized for their effectiveness in filtering both particulate and harmful vapors, however, most of these respirator types rely heavily on granulated activated carbon (GAC) as the primary vapor/gas adsorbent (Figure 1). A recent study suggested that incorporating activated carbon fiber (ACF) into a surgical mask may help reduce exposure to chemical constituents of surgical smoke during laparoscopic surgeries (Choi et al. 2018). First responders and the public could also be at risk of dual exposures in certain situations, such as during chemical spills or releases, and wildfires (Navarro et al. 2021). Wildfires are a growing concern as they release a complex mixture of pollutants, including PM, VOCs, and polycyclic aromatic hydrocarbons (PAHs). Research has indicated that exposure to wildfire smoke resulted in a notable increase in emergency department visits for cardiovascular and cerebrovascular issues in California (Wettstein et al. 2018).

There is a need for a particulate-vapor media that can be incorporated in FFRs for dual protection against VOCs and PM that would be optimal for short-term occupational tasks or emergency situations for workers in various occupations. Activated carbon fiber presents a viable option for providing dual protection against both particulate matter and vapor exposure due to its non-woven fiber structure and adsorption properties. Activated carbon fiber has the potential to serve as a lightweight alternative for dual-protection, benefiting not only workers but also the public. Activated carbon fibers are made by carbonizing organic precursor fibers (typically polyacrylic nitrate [PAN], or other synthetic polymers such as Rayon) using intense heat, inert and oxidizing atmospheres, and steam or carbon dioxide as the activation agent. This process creates a material with a high surface area capable of supporting VOC adsorption and particle filtration in the non-woven form.

Based on previous research, ACF has demonstrated considerable potential as a media for dual-purification against PM and gas/vapor (Chinn M et al. 2002; Chinn MHC and Pears L. 2002; Lorimier et al. 2008). However, existing studies have primarily focused on its adsorption capabilities, with limited focus on its dual-air purifying properties (Chinn MHC and Pears L. 2002; Lu 2005; Balanay et al. 2011; 2015; Clinger and O'Shaughnessy 2019; Khayan et al. 2019; Okrasa et al. 2019; Muzarpar et al. 2021; Summers et al. 2022). The limited research may be due to the unique interplay between VOCs and PM, altering the overall adsorption mechanisms of ACF. Previous research observed that the adsorption dynamics of VOCs onto PM are influenced by the chemical characteristics of both the VOCs and PM, which indicated that the existence of functional groups on PM may either enhance or inhibit VOC adsorption (Zhang et al. 2020). Although significant research has been conducted on the individual behavior of ACF with VOCs and PM, the precise interactions involved when both are present have not been thoroughly examined.

This study sought to examine the adsorption and filtration efficiency (FE) of ACF by conducting measurements in a sequential manner rather than

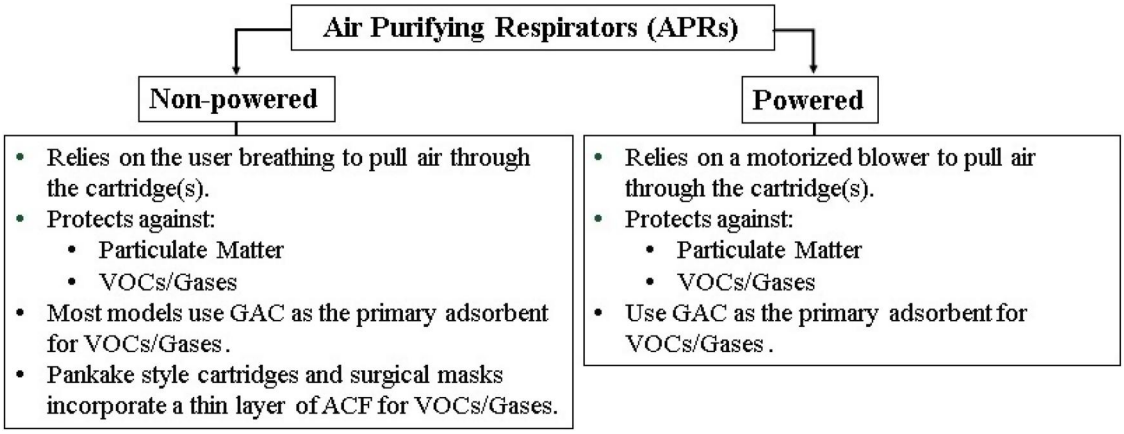

Figure 1. Categories of air purifying respirators.

simultaneously. By initially exposing the ACF to VOC, followed by PM, and subsequently reversing this experimental sequence, the study aimed to understand the underlying mechanisms governing the adsorption and filtration processes of activated carbon in the non-woven fiber form. This interaction is an important aspect to examine if ACF is to be used as particulate-vapor media.

Methods

ACF selection

A commercially available non-woven ACF felt with a nominal surface area of 1200 mg/m^3 was used in this study. It is manufactured with a PAN precursor using the electrospinning process. ACF 1200 was chosen for this study because of its high surface area, low pressure drop, and promising filtration capability based on previous studies (Lu 2005; Balanay et al. 2011; 2015; Balanay and Lungu 2016; Clinger and O'Shaughnessy 2019; Summers 2022; Summers et al. 2022).

ACF surface area characterization

To measure surface area and characterize the micropores of the ACF in the pristine (off-the-shelf) state, and after each experimental sequence (PM-VOC and VOC-PM), the ACF was subjected to nitrogen adsorption at 77 K utilizing a Micromeritics ASAP 2020 Physisorption Analyzer (Micromeritics Corp, Norcross, GA). The specific surface area and the average pore diameter of the ACF were determined using the Brunauer-Emmett-Teller (BET) method. The BET method measures the amount of nitrogen adsorbed at different pressures on the ACF's surface and is widely used to estimate the surface area of microporous carbon materials (Webb et al. 1997).

Test conditions

Test conditions for both challenge contaminants, PM and VOC, were maintained in a dynamic experimental set-up. The average recorded temperature was 22 ± 0.6 °C with a relative humidity (RH) at 50% ± 17%. An air flow rate of 7.5 standard liters per minute (SLPM) was maintained to carry the contaminant through the media. The flow rate was set based on a scaled-down approximation of the face velocity of the average respirator surface area of 100 cm^2 when a flow rate of 64 SLPM was used. Using a scaled-down approximation flow rate is the most appropriate approach to conform to the standard testing conditions required for certifying OV respirator cartridges in accordance with 42 Code of Federal Regulations (CFR) Part 84.207 Bench Tests for Gases and Vapors; Minimum General Requirements) (42 C.F.R., Part 84, 2004). Based on the test chamber dimensions, a face velocity of 10 cm/s was used to test the ACF during both particulate and VOC experiments.

Challenge contaminants

Particulate challenge

To generate a poly-dispersed sodium chloride (NaCl) aerosol, a 2% NaCl solution (Fisher Chemical, Fair Lawn, NJ) was added to the reservoir of a constant output atomizer (TSI Inc., Shoreview, Minnesota). The National Institute for Occupational Safety and Health (NIOSH) procedure TEB-APR-STP-0059 Determination of Particulate Filter Efficiency Level for N95 Series Filters Against Solid Particles for Non-powered Respirators) recommends a count median diameter (CMD) of 0.075 ± 0.020 µm with a geometric standard deviation of (GSD) <1.86 (equivalent to ~0.3 µm mass median diameter [MMD]) for the particle distribution (Jones and Rempel 2021). The concentration of the NaCl solution was validated by the manufacturer (TSI). A solution comprising 4 g of NaCl dissolved in 1,000 mL of deionized water was used for all experiments. The constant output atomizer was supplied with 20 psi of filtered compressed air. The generated aerosol passed through a diffusion dryer (TSI Inc., Shoreview, Minnesota) to remove moisture. The dried aerosol entered a Krypton-85 charged neutralizer (TSI Inc., Shoreview, Minnesota) before being dispersed into the mixing chamber. During each experiment, the aerosolized NaCl concentration (mg/m^3) in the mixing chamber was measured and had an average concentration of 215 ± 17 mg/m^3.

VOC challenge

Toluene (Fisher Chemical, Fair Lawn, NJ) was selected as a representative organic vapor due to its widespread use in solvents, paints, and coatings as well as its similarity to benzene, a human carcinogen. For the challenge concentration, 200 ppm was used, which is the Occupational Safety and Health Administration (OSHA) Permissible Exposure Limit (PEL). To create the vapor challenge, a separate filtered and metered compressed air line leading to a syringe pump (CHEMYX Inc., Stafford, TX) and mass flow meter (Sierra Instruments, Monterey, CA) was used. The

syringe pump constantly injected 0.50 ml/h of laboratory-grade toluene into the air stream to maintain a constant 200 ppm upstream concentration in a 7.5 SLPM of airflow.

Statistical analysis for toluene 10% breakthrough, filtration efficiency, pressure drop, and surface area

To determine whether there was a statistically significant difference in the experimental sequences (VOC-PM and PM-VOC) and across ACF layer combinations, a statistical analysis employing a significance level of ($\alpha = 0.05$) was conducted, focusing on concentration breakthrough times, filtration efficiency, pressure drop, and surface area. The Mann-Whitney U statistical nonparametric test was used due to small groups and the absence of normal distribution. The statistical software used to analyze data is JMP 18 (SAS Institute, Cary, NC).

Experimental Set-up

Particulate filtration and VOC breakthrough challenge experiments were conducted using the experimental set-up seen in Figure 2. The 1-, 2-, 3-, and 4-layer combinations of ACF 1200, and 1-layer of polypropylene downstream to prevent shedding (Figure 3), were placed in a stainless-steel test chamber with an external diameter of 6 cm. The media was secured between two circular chucks that have an internal diameter of 4 cm, a tapered inlet, and an expansion section that has an internal diameter >2 cm from the inlet to the material. Filter bypass was avoided by a firmly fitted threaded component on top of the media (Figure 4).

The experiments exposed the ACF 1200 to PM and toluene, however filtration and adsorption measurements were taken in sequence. The first set of experiments measured VOC breakthrough concentration, followed by FE. The second set of experiments measured FE first, followed by VOC breakthrough concentration. For the 1-, 2-, 3-, and 4-layer configurations of ACF 1200, each experimental sequence (VOC-PM and PM-VOC) was conducted six times ($n = 6$) for every number of layers, and the results were averaged.

Pressure drop measurements

Pressure drop (PD) denotes the resistance encountered across a filter medium during the processes of inhalation and exhalation. According to 42 CFR Part

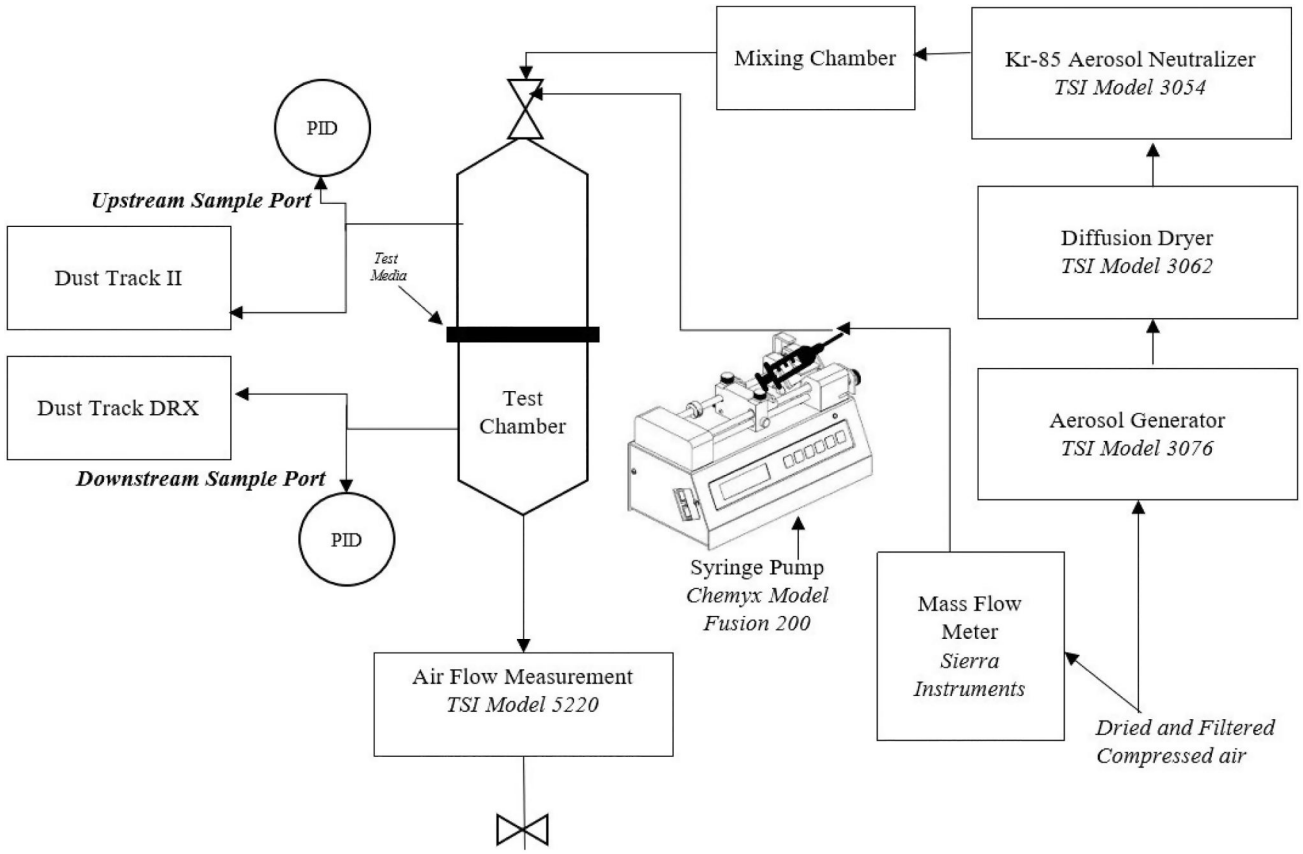

Figure 2. Experimental set-up.

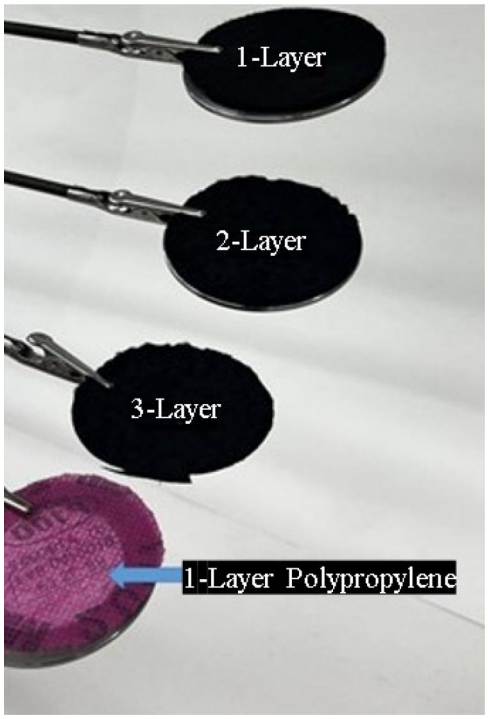

Figure 3. Layer combination.

Figure 4. Dynamic adsorption test chamber.

84.203 Breathing Resistance Rest; Minimum Requirements), OV respirators must not exceed a pressure drop of 40 mm H_2O during inhalation and 25 mm H_2O during exhalation (42 C.F.R., Part 84, 2004). The measurement of pressure drop was conducted using an anemometer equipped with a built-in manometer (TSI VelociCalc 8355, Shoreview, Minnesota), and differential pressure probes were employed to assess the pressure drop across the layer combinations of ACF (42 C.F.R., Part 84, 2004).

Filtration efficiency

The test chamber's upstream and downstream ports were connected to a TSI Model 8530 DustTrak II aerosol monitor (TSI Inc., Shoreview, Minnesota). The mass concentrations of particulate matter measured (mg/m^3) at both the upstream and downstream locations were used to determine the filtration efficiency through the application of the following equation:

$$Filtration\ Efficiency\ (\%) = \frac{(C_{up} - C_{down})}{C_{up}} X\ 100 \quad (1)$$

where C_{down} = *downstream mass concentration* (mg/m^3)
C_{up} = *upstream mass concentration* (mg/m^3)

VOC breakthrough measurements

The gas concentration was monitored via two VOCTraq II Photoionization Detectors (PID) (AMETEK MOCON Baseline, Lyone, CO) that individually measured upstream and downstream concentrations of toluene. The adsorption performance of ACF under dynamic use conditions is described by the Wheeler-Jonas (WJ) equation, a semi-empirical breakthrough time model used to determine the adsorption capacity of porous media based on first-order reaction kinetics. A 10% (0.10) breakthrough fraction was selected due to its reliability and established application in the assessment of carbon bed breakthrough (Wood 2000, 2002; Wu et al. 2005; Marsh and Reinoso 2006; Vizhemehr et al. 2014; Kempisty et al. 2020). The 10% breakthrough measurement was assessed for 1-, 2-, 3-, and 4-layer combinations of ACF using a PID. When written in terms of breakthrough time, the WJ equation is:

$$t_b = \frac{W_e\ W}{C_o Q} - \frac{W_e\ \rho_b}{C_o k_v} \times \ln\left(\frac{C_x}{C_o}\right) \quad (2)$$

where
t_b = *breakthrough time (min),*
W_e = *kinetic adsorption capacity (g/g),*
W = *weight of adsorbent (g),*
C_x =*outlet concentration* (g/cm^3),
C_o =*inlet concentration* (g/cm^3), *and*
Q = *volumetric flow rate* (cm^3/min).
k_v =*rate of constant adsorption* (min^{-1})
ρ_b =*density of the packed bed* (g/cm^3)

For each experimental sequence (PM-VOC and VOC- PM), a plot was constructed with the successive bed depths (layers) to illustrate the relationship

between the 10% breakthrough time (t_b) and bed weight (W, which is dependent on bed depth) (see Figures 5 and 6). The adsorption capacity (W_e) of the ACF was subsequently calculated from the plot utilizing the WJ equation, as detailed below:

$$W_e = slope \times C_o \times Q \quad (3)$$

where

W_e *=kinetic adsorption capacity (g/g),*

C_o *=inlet concentration (g/cm^3), and*

Q *= volumetric flow rate (cm^3/min).*

Adsorption capacity, W_e (grams contaminants/grams sorbent), was then determined for each experimental sequence (PM-VOC and VOC-PM).

Results

Breakthrough times by layer and experimental sequence (Figures 5 and 6) indicated that ACF 1,200 had a slightly higher adsorption capacity (g/g) for toluene when PM was present versus when it was not

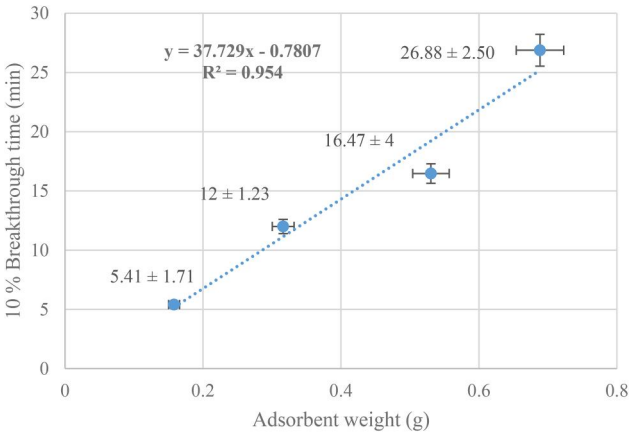

Figure 5. Breakthrough time plot for each ACF layer combination exposed to toluene before exposure to PM.

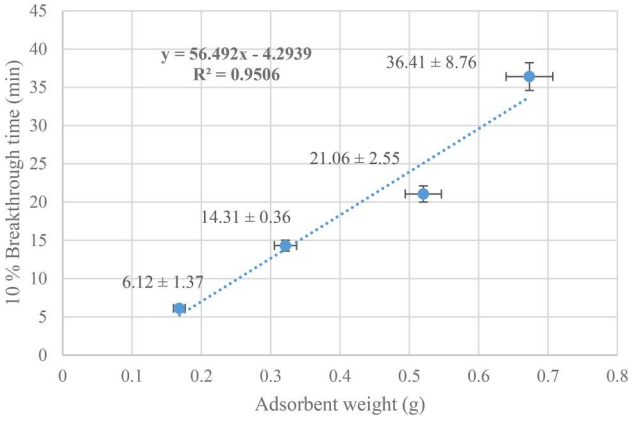

Figure 6. Breakthrough time plot for each ACF layer combination exposed to PM before exposure to toluene.

(0.319 g/g, 0.213 g/g, respectively), as seen in Table 1. Average 10% breakthrough times for 1-, 2-, 3-, and 4-layers of ACF prior to being exposed to PM were 5.41 ± 1.7, 12 ± 1.2, 16.4 ± 4, and 28.88 ± 2.5 min, respectively. Similarly, average 10% breakthrough times for the ACF exposed to PM before introducing VOC were 6.12 ± 1.3, 14.31 ± 0.3, 21.06 ± 2.5, and 36.41 ± 8.7 min, respectively, as seen in Table 1 and Figure 7. When comparing the concentration breakthrough times for the 1-, 2-, 3-, and 4- layer combinations according to experimental sequence (VOC-PM vs. PM-VOC), the *p-values* were $p = 0.150$, $p = 0.004$, $p = 0.025$, and $p = 0.002$, respectively. When combining all layers, the average concentration breakthrough times for the VOC- PM sequence (15.12 ± 8.3 min) and the PM-VOC sequence (19.5 ± 12.14 min) were not significantly different ($p = 0.149$).

Average filtration efficiency measurements for 1-, 2-, 3-, and 4-layers of ACF in the presence of VOC were 41 ± 4%, 52 ± 4%, 56 ± 2%, and 64 ± 3%, respectively. Similarly, FE averages for ACF particulate exposure without the presence of VOC were 35 ± 3%, 55 ± 4%, 57 ± 4%, and 63 ± 3%, respectively (Figure 8). The *P-values* for FE for the experimental sequences (VOC-PM vs. PM-VOC) for 1-, 2-, 3-, and 4-layers were $p = 0.025$, $p = 0.262$, $p = 0.200$, and $p = 0.522$, respectively. When combining all layers, the average FE for the VOC-PM sequence (53 ± 9.10%) and the PM-VOC sequence (53 ± 11%) were not significantly different ($p = 0.885$).

The average PD measurements for 1-, 2-, 3-, and 4-layers of ACF exposed to VOC prior to PM were 1.20 ± 0.26, 3.20 ± 0.19, 5.90 ± 0.07, and 9.10 ± 0.19 mm H_2O, respectively. Similarly, PD averages for ACF particulate exposure without the presence of VOC were 1.40 ± 0.22, 3.70 ± 0.39, 6.40 ± 0.30, and 9.30 ± 1.4 mm H_2O, respectively (see Figure 9). When comparing the PD for the 1-, 2-, 3-, and 4- layer combinations according to experimental sequence (VOC-PM vs. PM-VOC), the *p-values* were $p = 0.150$, $p = 0.128$, $p = 0.006$, and $p = 0.128$, respectively. When combining all layers, the average PD for the VOC-PM sequence (2.2 ± 0.5 mm H_2O) and the average for the PM-VOC sequence (2.5 ± 1.1 mm H_2O) were not significantly different ($p = 0.364$).

Surface area and porosity analysis were performed to assess the change in surface area for 1-, 2-, 3-, and 4-layers for each experimental sequence (VOC-PM and PM-VOC). The surface area results for 1-, 2-, 3-, and 4-layers for the VOC-PM experiments were 679 m^2/g, 641.27 m^2/g, 634.88 m^2/g, and 619.86 m^2/g, respectively. The percent decrease in surface area for

Table 1. Breakthrough times and adsorption capacity (g/g), for each experimental sequence.

Experimental Sequence	Layer	Bed weight (g)	$tb_{10\%}$ (min)	Adsorption capacity (g/g)
ACF 1200 (VOC-PM)	1	0.15 ± 0.03	5 ± 1.7	
	2	0.31 ± 0.08	12 ± 1.2	0.213
	3	0.53 ± 0.03	16 ± 4.0	
	4	0.68 ± 0.02	26 ± 2.5	
ACF 1200 (PM-VOC)	1	0.16 ± 0.02	6 ± 1.3	
	2	0.32 ± 0.07	14 ± 0.3	0.319
	3	0.52 ± 0.01	21 ± 2.5	
	4	0.67 ± 0.05	36 ± 8.7	

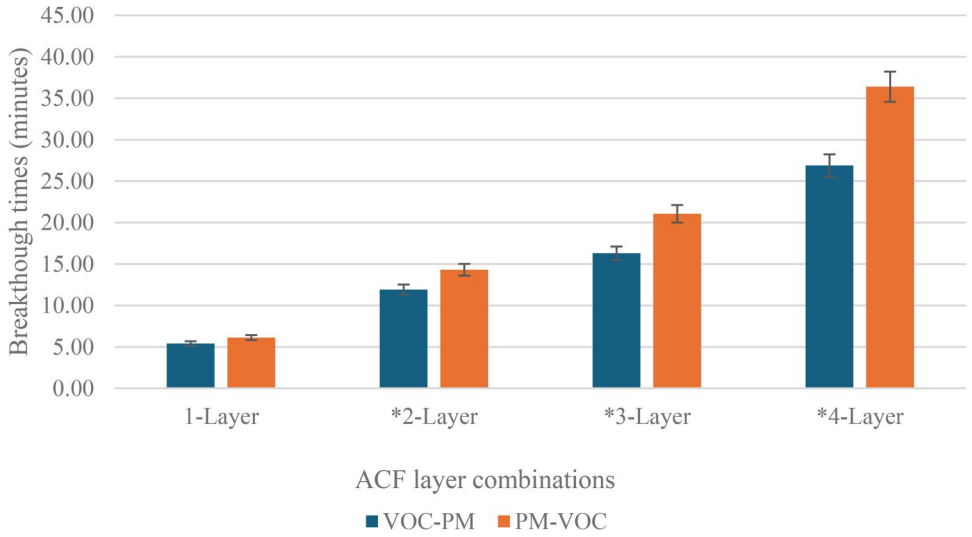

Figure 7. VOC breakthrough time comparison of layer combinations when first exposed to VOC or PM (* denotes statistical significance $p < 0.05$).

1-, 2-, 3-, and 4-layers for the VOC-PM experiments when compared to off-the-shelf ACF 1200 were 43.68%, 46.82%, 47.35%, and 48.60%, respectively. Similarly, the surface area results for 1-, 2-, 3-, and 4-layers for the PM-VOC experiments were 697.73 m^2/g, 656.51 m^2/g, 665.07 m^2/g, and 723.04 m^2/g, respectfully. The percent decrease in surface area for 1-, 2-, 3-, and 4-layers for the PM-VOC experiments were 42.14%, 45.56%, 44.85%, and 40.04%, respectively. The average percent change in surface area for VOC-PM (46.61 ± 2.09%) was significantly higher ($p = 0.021$) compared to PM-VOC (43.14 ± 2.54%).

Discussion

The study findings suggest that ACF 1200, when exposed to PM (aerosolized NaCl), may influence and enhance the adsorption mechanism of ACF. Comparative analysis of the two experimental sequences (VOC-PM and PM-VOC) indicated that aerosolized NaCl deposited on the ACF led to prolonged breakthrough times for toluene. Consequently, toluene adsorbed (g/g) during the PM-VOC sequence was 0.106 g/g higher (0.319 g/g) than the amount observed in the VOC-PM sequence (0.213 g/g).

Previous observations have shown that inorganic salts may enhance the adsorptive capacity of granular activated carbon by increasing pH and surface area, but this effect has not yet been investigated in the context of ACF in the fiber form (Horng 1990). Some studies suggest that the presence of aerosolized NaCl particles can significantly augment the adsorption mechanism of ACF for toluene. This could be a result of various synergistic interactions (Baur et al. 2015, Li et al. 2022).

The presence of NaCl may alter the surface properties and pore configuration of activated carbon, enhancing its overall adsorption capabilities (Baur et al. 2015). Other studies have suggested that the introduction of chloride ions can modify the surface charge and the functional groups present on the ACF, which increases its affinity for toluene (Zhao et al. 2024, Czerwinska et al. 2025). Notably, certain ions have been shown to enhance the adsorption of VOCs by fostering electrostatic interactions or hydrogen bonding between the toluene and the ACF (Li et al. 2022). This phenomenon is particularly significant for toluene, which, despite its non-polar nature, can still participate in weak interactions with the polar functional groups located on the surface of ACF.

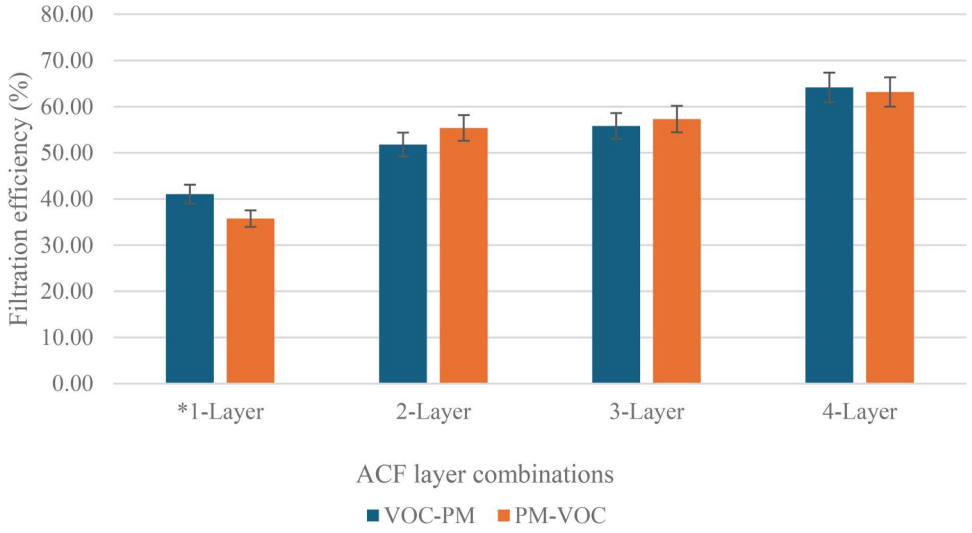

Figure 8. Filtration efficiency comparison of layer combinations when first exposed to VOC or PM (* denotes statistical significance $p < 0.05$).

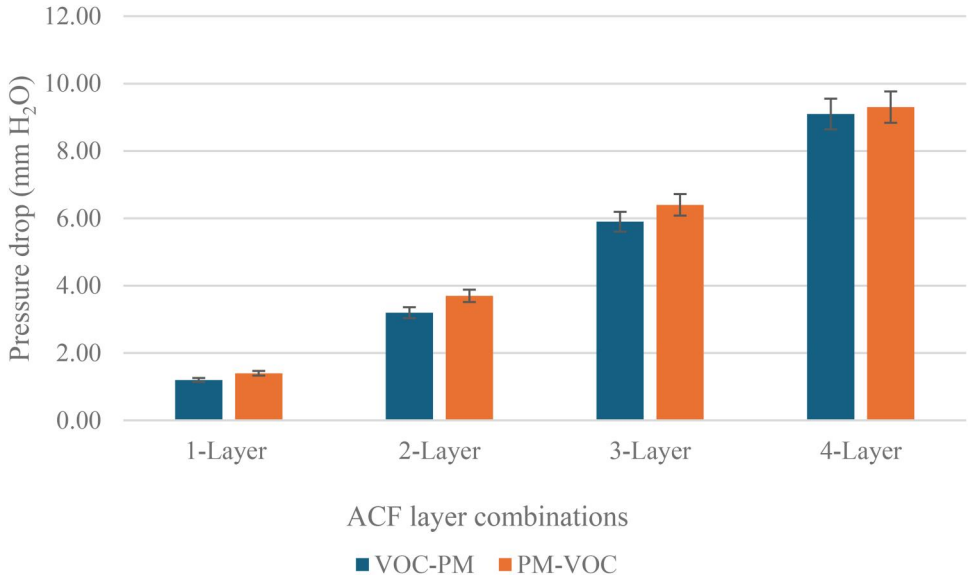

Figure 9. Pressure drop comparison of layer combinations when first exposed to VOC or PM.

There was statistical significance when comparing breakthrough times during experimental sequences (VOC-PM vs. PM-VOC) for 2-, 3-, and 4-layers; however, the VOC breakthrough time comparison of 1-layer of ACF was not significant (*p=.150).* Even though the *P-value* for 1-layer VOC breakthrough time was not statistically significant, it did correspond with the overall pattern of having a longer concentration breakthrough during the PM-VOC sequence. When combining layer combinations and only considering experimental sequence (VOC-PM vs. PM-VOC) for concentration breakthrough times, the *P-value* was insignificant (*p=.149).* Also, the presence of water vapor may compete with VOCs for available adsorption sites, adding complexity to adsorption behavior (Guo et al. 2021). This interaction between humidity and temperature can result in varying outcomes in repeated tests, as the experimental conditions may not be consistently reproduced in a dynamic scenario.

There was a decrease in FE for the 1 -layer of ACF following initial PM exposure, as seen in Figure 8. This may be attributed to a buildup of moisture on the ACF, which can cause degradation of the material, such as fiber swelling, leading to a reduction of its filtration capabilities (Tcharkhtchi et al. 2021). Research also suggests that moisture from PM in the form of aerosolized NaCl droplets may compete with toluene for available adsorption sites, resulting in a phenomenon known as competitive adsorption. In this scenario, the presence of moisture in PM can reduce the

overall effectiveness of the filtration mechanism of ACF and could hinder the adsorption of toluene (Li et al. 2022). Understanding these interactions is critical for the development of an FFR that aims to remove both VOCs and PM from contaminated air streams.

There was no notable change in pressure drop during the initial exposures to either VOC or PM. The pressure drop remained well below the NIOSH limit of 40 mm H_2O (inhalation) and 25 mm H_2O (exhalation) (Informed Consent 2004). This indicates that more layers can be added to augment FE without compromising breathing resistance.

Surface area analysis showed a decrease in surface area for each layer combination for each experimental sequence (VOC-PM and PM-VOC). The percent decrease in surface area for 1-, 2-, 3-, and 4-layers for the VOC-PM experiments was lower than the PM-VOC experiments (p=.021). The ACF (VOC-PM sequence) had more adsorption sites available than the ACF (PM-VOC sequence) after the experiments. The decrease in surface area that has been observed in the ACF following exposure to toluene prior to the introduction of NaCl can be explained by the distinct chemical interactions and physical changes that take place during these exposures. The differences in the surface area for both experimental sequences (VOC-PM and PM-VOC) are attributed to the chemical nature of toluene, which modifies the surface through the deposition of functional groups, leading to a reduction in surface area, while sodium chloride does not cause such changes.

Studies indicate that exposure to toluene on ACF can lead to the development of C-H stretching bonds, potentially resulting in a reduction of available surface area (Shakerinasab et al. 2024). This reduction may be attributed to the obstruction of pores and/or changes in the structure of the fibers (Shakerinasab et al. 2024). Research also suggests that the impact of aerosolized NaCl on the surface properties of ACF seems to diverge from that of toluene. Although NaCl does not notably increase the surface area of ACF, it has the potential to improve the adsorption of VOCs, without causing substantial surface modifications (Singhal and Kalra 2015; Akia et al. 2018).

Limitations

Recognized limitations of this study are the small sample size for the 1-, 2-, 3-, and 4-layer combinations tested against both experimental sequences (VOC-PM and PM-VOC). Utilizing a greater sample size in the assessment of the ACF layer combinations for each experimental sequence (VOC-PM and PM-VOC) could lead to an increase in statistical power.

The adsorption capacity (g/g), which is calculated from the plot utilizing the WJ equation is only able to be generated for each experimental sequence (two numbers); it is not possible to establish statistical significance with two numbers. This was a known limitation.

Another limitation was that the study used only toluene as a representative VOC. Toluene is a non-polar compound, so it cannot be generalized for other non-polar VOCs like Xylene and n-Hexane, or polar VOCs such as Methyl Ethyl Ketone (MEK).

The exact aerosol size distribution was not known; the NaCl particle size distribution was only known from previous studies. A dynamic experimental set-up was a limitation due to experiments being conducted in a fume hood, and because precise control of temperature and RH was not possible.

The authors acknowledge that the TSI DustTrak II was calibrated using a different aerosol from the NaCl used in this study, and accuracy could be affected. However, as mentioned before, the FE accuracy by itself was not the object of this study, but rather if changes in the measured FE of the ACF occur when the PM-VOC and VOC-PM sequence are applied. The authors acknowledge this as a limitation of our study.

Conclusions

This study provides evidence that aerosolized NaCl may enhance the adsorption capacity of ACF for toluene when NaCl is introduced prior to VOC. This conclusion is based on longer toluene breakthrough times observed when exposed to PM before exposure to toluene. The adsorption rates for toluene in the PM-VOC sequence appeared to be higher. However, this cannot be said with certainty due to the inability to perform a statistical analysis based on the WJ equation model providing only two numbers for adsorption capacity for each treatment (PM-VOC and VOC-PM). The ACF's surface area decreases with exposure to toluene and NaCl. There was a decrease in FE when ACF was exposed to VOC before exposure to particulate matter.

These findings underscore the importance of understanding the interactions between PM and VOC for the purpose of optimizing ACF as dual air purifying media. The results indicate that the incorporation of ACF into FFRs may have the potential to offer a

lightweight alternative for protection against particulate-vapor exposure in short-term or emergency situations. This research sets the stage for future work in developing a combined particulate-vapor FFR that utilizes ACF.

Recommendations

To enhance the FE of ACF 1200 without adversely affecting PD and VOC retention, it may be essential to explore the addition and evaluation of supplementary layers, such as melt-blown and electrostatically charged polypropylene. Future research should focus on testing the ACF against other non-polar VOCs, such as Xylene and n-Hexane, and polar VOCs like MEK, particularly the interaction and potential enhanced adsorption performance of the ACF in the presence of PM.

Expanding the research on ACF with different VOCs and PM is essential for gaining comprehensive insights into the performance of ACFs in diverse hazardous work environments. This approach is crucial for the comprehensive development of dual-air purifying media to be used in an FFR.

Disclosure statement

No potential conflict of interest was reported by the author(s).

Funding

This work was supported by the National Institute for Occupational Safety and Health [5T42OH008436-20].

Data availability statement

The authors agree to make data available to the publisher upon reasonable request.

References

Akia M et al. 2018. High-throughput production with improved functionality and graphitization of carbon fine fibers developed from sodium chloride-polyacrylonitrile precursors. Polymer Eng Sci. 58(11):2047–2054. https://doi.org/10.1002/pen.24816

Balanay JAG, Crawford SA, Lungu CT. 2011. Comparison of toluene adsorption among granular activated carbon and different types of activated carbon fibers (ACFs). J Occup Environ Hyg. 8(10):573–579. https://doi.org/10.1080/15459624.2011.613346

Balanay JAG, Floyd EL, Lungu CT. 2015. Breakthrough curves for toluene adsorption on different types of activated carbon fibers: application in respiratory protection. Ann Occup Hyg. 59(4):481–490. https://doi.org/10.1093/annhyg/meu105

Balanay JAG, Lungu CT. 2016. Determination of pressure drop across activated carbon fiber respirator cartridges. J Occup Environ Hyg. 13(2):141–147. https://doi.org/10.1080/15459624.2015.1091960

Baur GB, Beswick O, Spring J, Yuranov I, Kiwi-Minsker L. 2015. Activated carbon fibers for efficient VOC removal from diluted streams: the role of surface functionalities. Adsorption. 21(4):255–264. https://doi.org/10.1007/s10450-015-9685-5

Bernstein D, Suojalehto H. 2011. Occupational asthma: Etiologies and risk factors. Allergy Asthma Immunol Res. 3(3):157–167. https://doi.org/10.4168/aair.2011.3.3.157

Chen H, Lin M, Chen C, Liu H. 2011. Assessments of PAHs exposure and health effects for foundry's workers. Epidemiology (Fairfax). 22(1):S231–S232. https://doi.org/10.1097/01.ede.0000392398.82030.f0

Chinn MH,C, Pears L. 2002. Combined fibers for combined vapor and particulate filtration journal of the international society for respirator protection. Paper presented at: 2002 International Society for Respirator Protection Conference; Edinburgh, Scottland.

Choi SH et al. 2018. Activated carbon fiber filters could reduce the risk of surgical smoke exposure during laparoscopic surgery: application of volatile organic compounds. Surg Endosc. 32(10):4290–4298. https://doi.org/10.1007/s00464-018-6222-0

Clinger JC, O'Shaughnessy PT. 2019. Breakthrough analysis for filtering facepiece respirators impregnated with activated carbon. J Occup Environ Hyg. 16(7):423–431. https://doi.org/10.1080/15459624.2019.1594838

Collaborators GOCRRF. 2020. Global and regional burden of chronic respiratory disease in 2016 arising from non-infectious airborne occupational exposures: a systematic analysis for the Global Burden of Disease Study 2016. Occup Environ Med. 77(3):142–150. https://doi.org/10.1136/oemed-2019-106013

Czerwinska N et al. 2025. Electrospun fibers from biobased and recycled materials for indoor air quality enhancement. Molecules. 30(6):1214. https://doi.org/10.3390/molecules30061214

Guo X et al. 2021. Functionalized activated carbon for competing adsorption of volatile organic compounds and water. ACS Appl Mater Interfaces. 13(47):56510–56518. https://doi.org/10.1021/acsami.1c18507

Gutierrez AMJA, Galang MD, Seva RR, Lu MC, Ty DRS. 2014. Designing an improved respirator for automotive painters. Int J Ind Ergon. 44(1):131–139. https://doi.org/10.1016/j.ergon.2013.11.004

Hamanaka RB, Mutlu GM. 2018. Particulate matter air pollution: effects on the cardiovascular system. Front Endocrinol (Lausanne). 9:680. https://doi.org/10.3389/fendo.2018.00680

Horng P-Y. 1990. Effect of inorganic salts on adsorption process [D.Eng.Sc. dissertation]. New Jersey Institute of Technology.

Informed Consent. 2004. Title 42 C.F.R. Part 84: approval of respiratory protection devices.

Jayjock M, Levin L. 1984. Health hazards in a small automotive body repair shop. Ann Occup Hyg. 28(1):19–29. https://doi.org/10.1093/annhyg/28.1.19

Jones RM, Rempel D. 2021. Standards for surgical respirators and masks: relevance for protecting healthcare workers and the public during pandemics. Ann Work Expo Health. 65(5):495–504. https://doi.org/10.1093/annweh/wxab008

Kempisty DM et al. 2020. Granular activated carbon adsorption of carcinogenic volatile organic compounds at low influent concentrations. J Am Water Works Assoc. 1(2):e1128. https://doi.org/10.1002/aws2.1128

Khayan K, Anwar T, Wardoyo S, Lakshmi Puspita W. 2019. Active carbon respiratory masks as the adsorbent of toxic gases in ambient air. J Toxicol. 2019:5283971–5283977. https://doi.org/10.1155/2019/5283971

Kogevinas M et al. 2007. Exposure to substances in the workplace and new-onset asthma: an international prospective population-based study (ECRHS-II). Lancet. 370(9584):336–341. https://doi.org/10.1016/S0140-6736(07)61164-7

Li J et al. 2022. Effect of nitrogen functional groups on competitive adsorption between toluene and water vapor onto nitrogen-doped spherical resorcinol-formaldehyde resin-based activated carbon. Environ Sci Pollut Res Int. 29(56):85257–85270. https://doi.org/10.1007/s11356-022-21179-w

Lorimier C, Le Coq L, Subrenat A, Le Cloirec P. 2008. Indoor air particulate filtration onto activated carbon fiber media. J Environ Eng. 134(2):126–137. https://doi.org/10.1061/(ASCE)0733-9372(2008)134:2(126)

Lu H. 2005. Evaluation of activated carbon fibers (ACF) for removal of volatile organic compounds (VOCs) in indoor environments [dissertation]. Purdue University.

Marsh H, Reinoso FR. 2006. Activated carbon. Elsevier Science Publications. https://doi.org/10.1016/B978-0-08-044463-5.X5013-4

Muzarpar MS et al. 2021. The adsorption mechanism of activated carbon and its application—a review. Int J Adv Technol Mech Mechatron Mater. 1(3):118–124. https://doi.org/10.37869/ijatec.v1i3.37

National Academies of Sciences, Engineering, and Medicine. 2022. Respiratory protection in the workplace. In: Yost OC, Downey A, Samet J, editors. Frameworks for protecting workers and the public from inhalation hazards. Washington, DC: The National Academies Press. p 127–150. https://doi.org/10.17226/26372

Navarro KM et al. 2021. Exposure to particulate matter and estimation of volatile organic compounds across wildland firefighter job tasks. Environ Sci Technol. 55(17):11795–11804. https://doi.org/10.1021/acs.est.1c00847

Okrasa M et al. 2019. Adsorption performance of activated-carbon-loaded nonwoven filters used in filtering facepiece respirators. Int J Environ Res Public Health. 16(11):1973. https://doi.org/10.3390/ijerph16111973

Pongboonkhumlarp N, Jinsart W. 2022. Health risk analysis from volatile organic compounds and fine particulate matter in the printing industry. Int J Environ Sci Technol (Tehran). 19(9):8633–8644. https://doi.org/10.1007/s13762-021-03733-0

Shakerinasab E, Bavi EP, Balagna C, Ferraris M. 2024. A promising method for promoting interfacial adhesion of aramid/rubber composite using atmospheric pressure plasma surface modification. Polym Compos. 45(8):6950–6969. https://doi.org/10.1002/pc.28240

Shiraiwa M et al. 2017. Aerosol health effects from molecular to global scales. Environ Sci Technol. 51(23):13545–13567. https://doi.org/10.1021/acs.est.7b04417

Singhal R, Kalra V. 2015. Using common salt to impart pseudocapacitive functionalities to carbon nanofibers. J Mater Chem A. 3(1):377–385. https://doi.org/10.1039/C4TA05121A

Summers M. 2022. The fibrous disposition of ACF has been studied and shows the ablity to filtrate particulates and VOCs [dissertation].

Summers M, Oh J, Lungu CT. 2022. Determination of activated carbon fiber adsorption capacity for several common organic vapors: applications for respiratory protection. J Air Waste Manag Assoc. 72(6):570–580. https://doi.org/10.1080/10962247.2021.1985013

Tagiyeva N et al. 2017. Occupational airborne exposure in relation to Chronic Obstructive Pulmonary Disease (COPD) and lung function in individuals without childhood wheezing illness: a 50-year cohort study. Environ Res. 153:126–134. https://doi.org/10.1016/j.envres.2016.11.018

Tcharkhtchi A et al. 2021. An overview of filtration efficiency through the masks: mechanisms of the aerosols penetration. Bioact Mater. 6(1):106–122. https://doi.org/10.1016/j.bioactmat.2020.08.002

Vizhemehr AK, Haghighat F, Lee C-S. 2014. Gas-phase filters breakthrough models at low concentration–Effect of relative humidity. Build Environ. 75:1–10. https://doi.org/10.1016/j.buildenv.2014.01.010

Webb PA, Orr C, Camp RW, Olivier JP, Yunes YS. 1997. Analytical methods in fine particle technology. Vol. 55. Micromeritics Instrument Corporation.

Wettstein ZS et al. 2018. Cardiovascular and cerebrovascular emergency department visits associated with wildfire smoke exposure in California in 2015. J Am Heart Assoc. 7(8):e007492. https://doi.org/10.1161/JAHA.117.007492

Wood GO. 2000. Reviews of models for adsorption of single vapors, mixtures of vapors, and vapors at high humidities on activated carbon for applications including predicting service lives of organic vapor respirator cartridges. Los Alamos National Laboratory LA-UR-00-1531 (March 2000).

Wood GO. 2002. Quantification and application of skew of breakthrough curves for gases and vapors eluting from activated carbon beds. Carbon N Y. 40(11):1883–1890. https://doi.org/10.1016/S0008-6223(02)00031-3

Wu J, Claesson O, Fangmark I, Hammarstrom L-G. 2005. A systematic investigation of the overall rate coefficient in the Wheeler–Jonas equation for adsorption on dry activated carbons. Carbon N Y. 43(3):481–490. https://doi.org/10.1016/j.carbon.2004.09.024

Zhang C, Wu Z, Li Z, Li H, Lin J-M. 2020. Inhibition effect of negative air ions on adsorption between volatile organic compounds and environmental particulate matter. Langmuir. 36(18):5078–5083. https://doi.org/10.1021/acs.langmuir.0c00109

Zhao Z et al. 2024. Thermosetting phenolic resin-derived activated carbon fibers for volatile organic compound adsorption: electrospinning, preoxidation, and carbonization. ACS EST Eng. 4(7):1635–1643. https://doi.org/10.1021/acsestengg.4c00060